Catena 150 (2017) 1–8

Contents lists available at ScienceDirect

Catena

journal homepage: www.elsevier.com/locate/catena

Laboratory characterization of rainfall-induced loess slope failure

L.Z. Wu [a], Y. Zhou [a], P. Sun [b,c,*], J.S. Shi [d], G.G. Liu [a], L.Y. Bai [a]

[a] State Key Laboratory of Geohazard Prevention and Geoenvironment Protection, Chengdu University of Technology, Chengdu, Sichuan 610059, China
[b] Institute of Geomechanics, Chinese Academy of Geological Sciences, Beijing 100081, China
[c] Key Laboratory of Neotectonic Movement and Geohazard, Ministry of Land and Resources, Beijing 100081, China
[d] China Geological Survey, M.L.R, Beijing 100037, China

ARTICLE INFO

Article history:
Received 26 May 2016
Received in revised form 13 October 2016
Accepted 2 November 2016
Available online 5 November 2016

Keyword:
Loess
Rainfall infiltration
Landslide
Flume experiment

ABSTRACT

Loess slopes are widely distributed throughout the northwestern region of China and are prone to slope failure in response to heavy rainfall. We undertook three groups of flume experiments in the laboratory to study loess slope dynamics under artificial rainfall conditions. Additionally, a laser scanner was used to observe loess landslide deformation characteristics and failure development. A numerical analysis of unsaturated seepage in loess slopes because of rainfall infiltration was performed. Moisture content, pore-water pressure, and slope deformation were monitored to quantify the relationship between rainfall infiltration and loess slope stability. Movement of the wetting front near the slope surface was triggered by rainfall and related to rainfall intensity and duration, which is consistent with the numerical solution. Rainfall infiltration increased pore-water pressure, producing gravity-driven landslides. We observed that landslide development began with local failure in the toe slope that gradually retreated toward the crown, forming a multi-sliding displacement, and eventually resulting in total slope failure.

1. Introduction

Loess is a silt-rich, aeolian soil that is widely distributed in the Chinese Loess Plateau covering at least 6.31×10^5 km^2, including Gansu, Ningxia, Shaanxi, Shanxi, and Henan provinces (Derbyshire et al., 2000). Loess hillslopes are particularly prone to landsides as a result of rainfall (Meng et al., 2000; Zhang and Liu, 2010; Wang et al., 2011; Xu et al., 2012; Wang et al., 2014a, 2014b; Peng et al., 2015; Shi et al., 2016).

Landslides can be triggered when water from rainfall or irrigation wets loess at a shallow depth (Brand, 1981; Anderson and Sitar, 1995; Sorbino and Nicotera, 2013), while the saturated zone simultaneously rises from depth (Dai et al., 1999). Increased water content decreases matric suction in partially saturated loess, and increases positive pore-water pressure in completely saturated loess, both of which decrease soil shear strength (Xu et al., 2013).

Though a full-scale field experiment involving artificial rainfall has already been conducted on a loess plateau (Tu et al., 2009), laboratory experiments provide additional benefits. They allow us to analyze soil deformation in a much shorter time, provided that the forces and dimensions are chosen based on suitable scaling methods (Rosenau et al., 2009). Another advantage of laboratory experiments is that boundary conditions are well known and controllable, allowing us to systematically investigate interacting factors (e.g., hydraulic stress state, slope inclination and soil structure) and their influence on deformation processes (Moriwaki et al., 2004; Ochiai et al., 2004; Okura et al., 2002; Wang and Sassa, 2003). Hydrological and laboratory models for identifying landslide-prone locations are developed by combining subsurface flow models and slope stability models (e.g., Wu and Sidle, 1995; Wilkinson et al., 2000; Casadei et al., 2003; Crosta and Frattini, 2003). The suitability of a laboratory-scale experiment can be judged by a combination of the accuracy, precision and resolution of the measurement system (White et al., 2003).

The objective of this study was to observe the deformation and failure of a laboratory-scale experimental loess slope using a laser scanning system while simultaneously measuring water content and pore-water pressure. SEEP/W is used to further analyze variation in wetting front and pore-water pressure during rainfall infiltrating into partially saturated loess slope. This enabled us to quantify variations in slope characteristics in response to rainfall and identify conditions that trigger landslides.

2. Methods

2.1. Experiment design

Loess was collected in Shaanxi Province (Fig. 1). Physical parameters of the test material are shown in Table 1. Considering

* Corresponding author at: Institute of Geomechanics, Chinese Academy of Geological Sciences, Beijing 100081, China.
E-mail address: sunpingcgs@163.com (P. Sun).

http://dx.doi.org/10.1016/j.catena.2016.11.002
0341-8162/

Fig. 1. A typical loess landslide at Shaanxi province, China.

the size-effect of the test model box, the loess sample was broken by hammer and passed through a 5 mm screen. Particle analysis shows that particle size of the loess main is from 5 to 50 μm. However, the tiny particles tend to bond together to form larger particles. The particle size of loess used in tests was mostly between 0.2 and 2 mm (Fig. 2). A three-dimensional experimental loess slope was constructed in a 1.2 m × 0.4 m × 0.6 m (length × width × height) box with glass sidewalls and a metal frame. The box was first filled with a 10-cm-thick loess layer, with subsequent layers being 5 cm thick. The experimental slope was constructed with a gradient of 60° (tests A and B) and 45° (test C) (Fig. 4, Table 2). Hydrologic sensors were installed at specific depths (Table 3) as the slope was constructed, including four EC-5 volumetric water content sensors with an accuracy of ±2% (Decagon, USA) (Fig. 3a, T1–4 in Fig. 4) and four MPS-6 matric suction sensors with an accuracy of ±10 kPa (Decagon, USA) (Fig. 3b, H1–4 in Fig. 4). The sensors were respectively connected to 2 Em50 data loggers (Decagon, USA) (Fig. 3c). The sensors were calibrated before each experiment.

Table 1
Physical properties of the loess used in this study.

Permeability coefficient (10^{-5} m/s)	Saturated density (kN/m^3)	Natural density (kN/m^3)	Saturated moisture content (%)	Initial moisture content (%)
7.4619	19.7	15.4	47.2	9.6

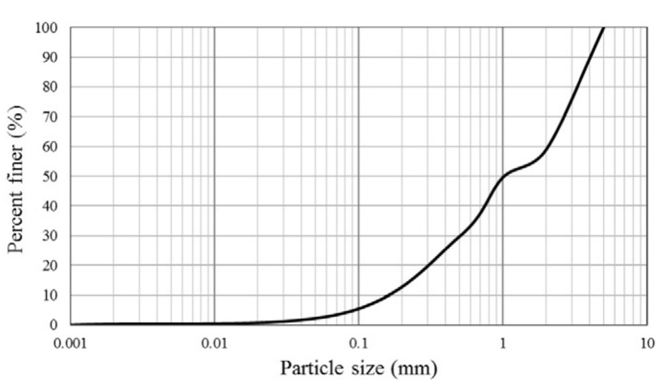

Fig. 2. Particle sizes of loess used in this study.

The experimental slope was placed under an artificial rainfall system, which has an effective rainfall area of 16 m^2 and can produce rainfall ranging in intensity from 20 to 260 mm/h. We used rainfall intensities of 45 and 70 mm/h (Table 2). Deformation was monitored using a 3D laser scanner (Leica Scanstation 2; Leica Geosystems, Heerbrugg, Switzerland) (Fig. 3d). The scanner can rapidly capture and record small-scale deformation of the loess slope with 1-mm precision. High-resolution topographic data were obtained by repeatedly scanning the slope surface every 30 min during each experiment. Polyworks (Version 10, InnovMetric, Canada) and Surfer software were used to process the data and quantitatively describe slope deformation and failure characteristics.

2.2. Experimental process

Our experimental scheme used two slope gradients and two rainfall intensities over three runs to separate their effects (Table 2). Prior to each experimental run, the slope was covered with a thin film for 24 h to avoid evaporation of slope moisture. Experiments did not start until all the sensors had stable readings. To run each experiment, the rainfall intensity was rapidly increased to the desired rate and allowed to run until the slope front had completely failed. Photographs were taken of the slopes throughout the experiment to supplement the topographic data.

Table 2
Test parameters of the loess slope model.

Test ID	Initial pore water pressure (kPa)	Initial moisture content (%)	Rainfall intensity (mm/h)	Gradient (°)	Height (cm)
A	−231.8	9.8	70	60	50
B	−267.2	9.5	45	60	50
C	−253.4	9.6	45	45	50

Table 3
Vertical depths of the four moisture sensors (T1–T4) for the three test (A–C).

Vertical depth (cm)	A	B	C
T1	10	10	10
T2	20	20	20
T3	12.7	12.7	15
T4	10.3	10.3	15